Low-Frequency Stimulation Induces Stable Transitions in Stereotypical Activity in Cortical Networks

Ildikó Vajda,*† Jaap van Pelt,* Pieter Wolters,¶ Michela Chiappalone,§ Sergio Martinoia,§ Eus van Someren,†‡ and Arjen van Ooyen*

*Department of Experimental Neurophysiology, Center for Neurogenomics and Cognitive Research, VU University Amsterdam, 1081 HV Amsterdam, The Netherlands; †Department of Sleep and Cognition, Netherlands Institute for Neuroscience, 1105 BA Amsterdam, The Netherlands; ‡Departments of Neurology, Clinical Neurophysiology and Medical Psychology, VU University Medical Center, Amsterdam, The Netherlands; §Department of Biophysical and Electronic Engineering, University of Genoa, 16145 Genoa, Italy; and ¶Department of Neurons and Networks, Netherlands Institute for Neuroscience, 1105 BA Amsterdam, The Netherlands

ABSTRACT Reverberating spontaneous synchronized brain activity is believed to play an important role in neural information processing. Whether and how external stimuli can influence this spontaneous activity is poorly understood. Because periodic synchronized network activity is also prominent in in vitro neuronal cultures, we used cortical cultures grown on multielectrode arrays to examine how spontaneous activity is affected by external stimuli. Spontaneous network activity before and after low-frequency electrical stimulation was quantified in several ways. Our results show that the initially stable pattern of stereotypical spontaneous activity was transformed into another activity pattern that remained stable for at least 1 h. The transformations consisted of changes in single site and culture-wide network activity as well as in the spatiotemporal dynamics of network bursting. We show for the first time that low-frequency electrical stimulation can induce long-lasting alterations in spontaneous activity of cortical neuronal networks. We discuss whether the observed transformations in network activity could represent a switch in attractor state.

INTRODUCTION

Synchronized activity among neurons occurs in many brain areas and is believed to be relevant for information processing (1), including sensory processing (2), cognition (3–5), and sleep (6,7). Patterns of reverberating synchronized activity are thought to reflect neuronal representations of cognitive processes and stored memories (8,9).

Synchronized neuronal activity is also observed in vitro. Cultures of dissociated cortical neurons, for example, exhibit stereotypical and spontaneously occurring patterns of reverberating synchronous activity. In these cultures, periods of network-wide depolarization, so-called network bursts, alternate with periods of relatively low activity (10–13). Network bursting closely resembles the ''up'' and ''down'' states of the intact cerebral cortex during slow-wave sleep (14). The persistence of such reverberating activity in cultures of dissociated cortical neurons, which lack the special wiring of the thalamocortical circuitry, suggests that it is an important intrinsic form of network activity. Besides its relevance for the mature brain, spontaneous activity also plays a role in the ontogeny of neuronal networks (15).

In cortical cultures, spontaneous activity and network bursting are usually studied without application of any external input. The intact brain, however, is massively bombarded with external and internal stimuli, which may modify the dynamics of spontaneous activity. Dissociated cortical cultures grown on multielectrode arrays are sensitive to external electrical stimulation (16–18). However, it is largely unknown whether external stimuli are capable of inducing long-term changes in the spatiotemporal patterns of spontaneous activity. A straightforward way to investigate this is by analyzing the stereotypical network activity before and after the application of electrical stimulation. Only one study attempted to do this using unphysiological, high-frequency tetanizing stimuli, but found no significant differences in spontaneous network bursting before and after stimulation (17). It has not been investigated how spontaneous activity and network bursting would respond to more physiological, low-frequency stimulation. In Eytan et al. (19) only relatively short-term effects of low-frequency stimulation were considered. Other studies (17,20,21) used low-frequency stimulation to probe the network before and after high-frequency tetanizing stimulation, but did not examine whether low-frequency stimuli themselves could already induce changes in activity patterns.

In this study, we applied external, low-frequency electrical stimuli to several electrode sites, and analyzed spontaneous activity and network bursting before and after stimulation. We report that low-frequency stimulation influenced greatly the pattern of spontaneous stereotypical network activity. The stable activity pattern was transformed into another stable pattern by serial, focal stimulation. The transformation consisted of changes in mean firing frequencies, both of the network as a whole and of single electrode sites; changes in

Submitted May 14, 2007, and accepted for publication January 23, 2008.

Address reprint requests to Jaap van Pelt or Arjen van Ooyen, Dept. of Experimental Neurophysiology, Center for Neurogenomics and Cognitive Research, VU University Amsterdam, De Boelelaan 1085, 1081 HV Amsterdam, The Netherlands. Tel.: 31-20-5987043 (J.v.P.), 31-20-5987090 (A.v.O); Fax: 31-20-5987112; E-mail: jaap.van.pelt@cncr.vu.nl, arjen.van.ooyen@cncr.vu.nl.

Editor: Herbert Levine.

0006-3495/08/06/5028/12 $2.00

doi: 10.1529/biophysj.107.112730

the shape of the mean network burst; and changes in the temporal structure of large network bursts. We discuss whether the transformation of network activity could reflect a switch in attractor state (22–24).

MATERIALS AND METHODS

Cell cultures

Cortical cells from embryonic (E17–18) rats were dissociated and plated on planar multi-electrode arrays (MEAs). Pregnant Wistar rats were anesthetized by CO_2 and decapitated according to a protocol approved by the Royal Dutch Academy of Arts and Sciences (ref. no. NIH05.26). Embryos were removed and kept on ice until decapitation. After decapitation, cortices were removed and dissociated according to the protocol described earlier in (25,26). The final plating medium consisted of Neurobasal medium, supplemented with B27 and penicillin/streptomycin (all from Invitrogen, Carlsbad, CA). The same medium was used for plating, culturing, and recording; $\sim 10^5$ cells were plated in a 50 μl drop into a glass ring (7 mm inner diameter) centered on the 60 electrode-MEAs, which were precoated with polyethylene-imine (PEI, 10 mg/ml, Fluka, Sigma-Aldrich, the Netherlands). This resulted in a plating density of $\sim$2600 cells/mm^2. After 1 h of incubation, 500 μl of the plating medium was added to the MEAs. Cultures were maintained at 35°C in an incubator with 5% CO_2 and 95% air. Half of the medium was replaced once weekly. MEAs were purchased from Multi-Channel Systems (MCS, Reutlingen, Germany) and consisted of titanium nitride electrodes with silicon nitride as insulation material. MEAs had either a hexagonal configuration with mixed 30, 20, and 10 μm electrode diameters (14 cultures) or an 8 $\times$ 8 configuration with 10 μm diameter (3 cultures).

Recording and stimulation systems

Electrical activity was recorded with the MEA 1060 preamplifier (MCS) relative to a glass reference electrode. Continuous analog traces from the amplifier were fed into a home-made 60-channel action potential (spike)-discrimination unit. Sampling took place at 22.2 kHz and spikes were detected by threshold discrimination. Thresholds were set automatically before measurements for each electrode at a factor of 1.9 times the median of 11 positive maximum electrode trace levels, measured in 11 successive 2 ms time bins (see Van Pelt et al. (11) for a more detailed description of the home-made recording system). Whenever the trace exceeded this threshold, a spike occurred and a time stamp, using a 10 kHz clock, was made for that electrode and stored on hard disk. For inspection of analog electrode traces, we used the MC Rack software of the MCS. This allowed us not only to visually check the quality of the noise bands and electrode traces, but also to record short episodes of analog traces from all channels.

For voltage stimulations of individual electrodes, the eight-channel MultiChannel Systems (MCS) stimulus generator was used (STG1008). Voltage waveforms were programmed using the accompanying MC Stimulus software. From the eight available channels of the stimulator, the first channel was always used for electrode stimulation. Different single electrodes were stimulated sequentially (see below).

Experimental protocol

Before experimentation, glass covers were put on top of the culture dishes to protect them against evaporation and to keep them sterile. All measurements were carried out at 37°C. The temperature of the culture was controlled by heating the preamplifier and adjusting the temperature if needed by a temperature controller (TCO2, MCS). The ages of the cultures ranged from 10 days in vitro to 54 days in vitro.

Cultures ($n = 17$) were placed in the preamplifier, and after 20–30 min of accommodation, spontaneous activity was measured for a period of at least 1 h. The main stimulation protocol consisted of a train of 40 low-frequency (0.2 Hz) biphasic rectangular voltage pulses (Fig. 1, *top row*) (positive first; 200 μs per phase; 1.5 V peak-to-peak, relative to reference electrode). The voltage pulse train was applied consecutively to six different electrodes. Before and after the application of the stimulus pulse train at a given electrode, spontaneous activity in the network was recorded for a period of $\sim$5 min (see, for instance, stimulation at sites *A* and *B* in Fig. 1, *center row*). The total stimulation protocol thus lasted $\sim$80 min (Fig. 1, *bottom row*). The amplitude of 1.5 V peak-to-peak turned out to be sufficient to evoke spikes in all cultures tested (I. Vajda, unpublished results). The stimulation sites were identical in each experiment. Thus, in each experiment, the same electrodes were stimulated in a fixed order with an equal number of pulses. After stimulating all six electrodes, at least 1 h of spontaneous activity was recorded after which the culture was put back in the incubator immediately.

Data collection and analysis

Time stamps of spikes from 60 recording sites were collected, and each spike event was labeled with a clock time running at 10 kHz and a bit pattern indicating at which sites action potentials had occurred. Spike analyses were carried out offline by a homemade software tool written in Fortran on a Linux platform and MATLAB (The MathWorks, Natick, MA) on a Windows platform. Recordings started $\sim$30 min after placing the cultures in the measuring setup. The stability of firing after such an accommodation period was tested off-line by comparing the mean firing rate in the first and the second half of the prestimulus period using a double sided *t*-test. Recordings that showed significantly different firing rates in these periods (95% confidence level) were excluded from further analysis (4 of 25).

Our aim was to quantitatively and qualitatively characterize spontaneous firing rate and network-wide bursting. Network bursting is the stereotypical firing behavior of dissociated cortical cultures and consists of periodic synchronized firing of many neurons. Spontaneous firing rate and network bursting was characterized before and after electrical stimulation using three main measures: 1), profile of the mean network burst; 2), characterization of the firing rate at single electrode sites; and 3), return plots of individual large network bursts to visualize the temporal structure of the bursts.

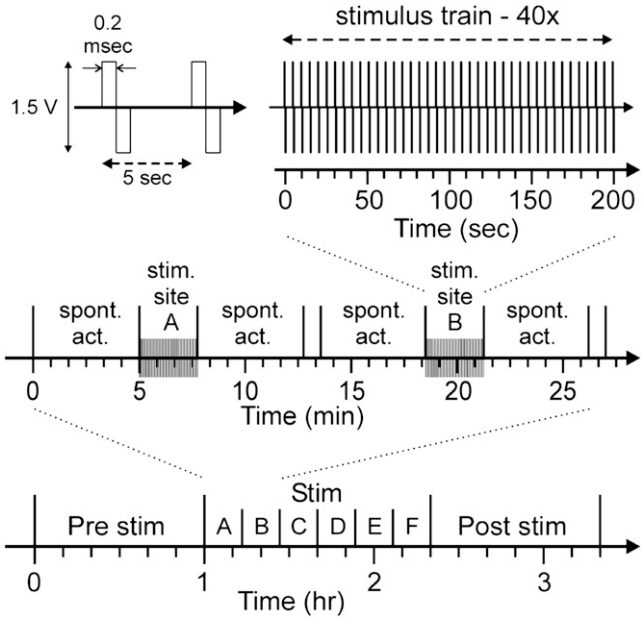

FIGURE 1 Scheme of the main stimulation protocol. Stimulated sites are indicated by capital letters; spont. act., spontaneous activity. See ''Experimental protocol'' for further description and details.

Profile of the mean network burst

A network burst is defined as an event of synchronized firing of many spatially dispersed neurons in the network (11,27,28). The criterion for detecting network bursts was described previously in detail (11,29). Briefly, network bursts were automatically detected off-line on the basis of periods of elevated firing rates and an increase in the number of active sites during such periods. In consecutive 25 ms time bins, the product of the number of active sites and the total number of spikes at these sites was calculated. Whenever this product exceeded a criterion value of 9 (that was shown previously to be adequate to capture network bursts; see Van Pelt et al. (11)), a network burst was considered to be encountered. Next, the bin for which the product is maximal was searched for among the adjacent bins. Finally, a more precise estimate of the center time of a burst was obtained by calculating the ''center-of-mass'' time point of the product distribution evaluated within a window of five bins left and right of the center bin.

The profile of the mean network burst was constructed as follows. First, around the center time of each network burst, in a time window of sufficient width to accommodate the network burst, spikes were searched across all channels and aggregated in time bins of 10 ms. The histograms of spike counts of all the network bursts were subsequently aligned to their center time points before they were added. The profile of the mean network burst was then obtained by averaging, for each bin, across all the different network bursts; the profile is thus expressed as spikes/burst/bin (see Fig. 9). The onset and termination of the mean network burst were determined after fitting an analytical function through the profile of the mean network burst. We used a function consisting of three components: a background, B, a double sigmoid function, $S(x)$, and a Gaussian component, $G(x)$. In this way, both the slower and the faster phase of the mean network burst profiles could be captured:

$$F(x) = B + S(x) + G(x), \tag{1}$$

where

$$B = a_1,\ S(x) = a_2 \times \frac{1}{1 + e^{(x-a_3)/a_4}} \times \frac{1}{1 + e^{(x-a_5)/a_6}}, \tag{2}$$

and

$$G(x) = a_7 \times e^{-\frac{(x-a_9)^2}{2a_8^2}}. \tag{3}$$

The background term is taken constant at a_1, representing the amplitude of the tonic background firing. The double sigmoidal function is the product of two sigmoidal functions (one for the rising phase, and the other for the falling phase) and describes a smooth function with tails that go to zero and a rising and falling phase with separate inflection points (a_3 and a_5, respectively) and steepness (a_4 and a_6, respectively). These four parameters, $a_3 - a_7$, describe a whole family of functions with varying widths, asymmetries, and steepnesses. The symmetric Gaussian function $G(x)$ centers at a_9 with standard deviation a_8. The fit function has nine free parameters, $a_1 - a_9$, that were all available for optimization. For the actual curve fitting, the routine ''mrqmin'' based on the Levenberg-Marquardt method as described by Press et al. (30) was used. An example of the procedure is shown in Fig. 2. Note that the fit function was chosen to optimally describe the shape of the network burst, without the intention of reflecting an underlying model of burst generation, as is done in Eytan and Marom (31).

To quantify the profile of the mean network burst, we took the duration of the rising phase (period between the left 5% point to the maximum), the duration of the falling phase (period from the maximum to the right 5% point) and the total duration (width) of the network burst (i.e., the rising phase plus the falling phase) (Fig. 2).

Characterization of the firing rate at single electrode sites

Scatter plots were used to compare mean firing rates at individual electrodes between two periods of spontaneous activity (Fig. 3). Each point in the scatter plot represents mean firing rates (spikes per minute) for two periods of spontaneous activity (period 1: x axis; period 2: y axis) on a single electrode. For ease of interpretation, the scatter plot is divided into six regions, which represent the following situations (Fig. 3): inactive (no activity in either of the two periods, i.e., lower than 0.1 spikes/min), activated (no activity in period 1 and activity in period 2, silenced (activity in period 1 and no activity in period 2, increased (higher activity in period 2 than in period 1, decreased (lower activity in period 2 than in period 1, and similar activity in both periods (region around the diagonal). This latter region is the region of confidence and is bounded by intervals of 3 SD in the firing rate, which were calculated on the basis of a Poisson distributed spike train. For a Poisson spike train with a firing rate R, the number of spikes in a given period T is distributed with mean RT and SD $\sqrt{RT}$. The firing rate in a given period T is distributed with the SD $\sqrt{RT}/T = \sqrt{R/T}$. The scatter plot representation makes immediately clear whether there are any differences in firing rates between the two periods. Data points outside the confidence region may indicate significant changes in spontaneous firing between period 1 and 2, and data points around the diagonal and within the confidence region may indicate no significant changes.

For each experiment, we compared the following periods of spontaneous activity: a), the first and the second half of the period before stimulation (see Fig. 7, *left panels*); b), the second half of the period before stimulation and the first half of the period after stimulation (see Fig. 7, *centrer panels*); and c), the first and the second half of the period after stimulation (see Fig. 7, *right panels*). As a control, comparisons between time periods of these durations were also made for recordings of spontaneous firing only, thus without stimulation.

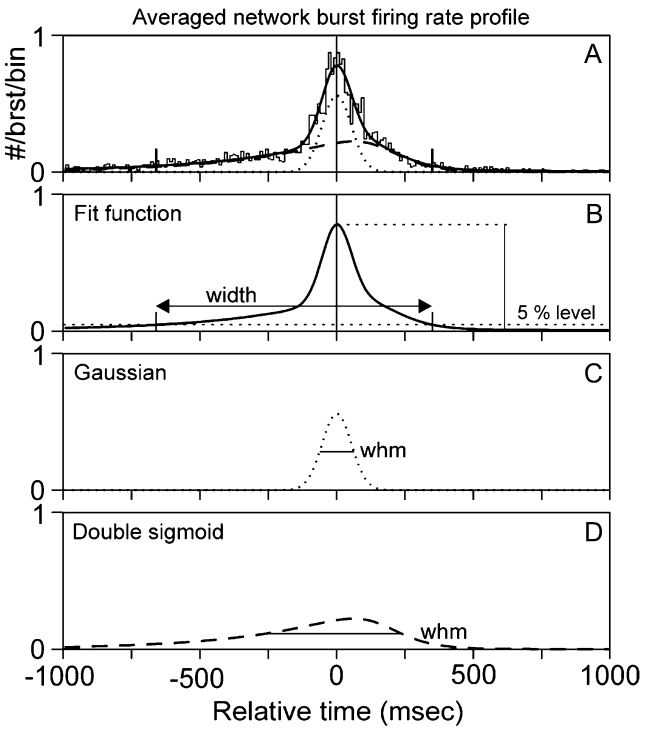

FIGURE 2 Firing rate profile of the averaged network burst. (*A*) Histogram of action potentials per burst per time bin of 10 ms. In this example, the average is taken over 133 network bursts detected in a period of 1 h. The optimized fit function (*solid line*) is composed of a double sigmoid function (*dashed line*), a Gaussian function (*dotted line*), and a background constant (not drawn). (*B*) Calculation of the width of the fit function from its crossings with the 5% level of the peak value. (*C*) The Gaussian component and its width at half-maximum level. (*D*) The double sigmoid function and its width at half maximum (*whm*).

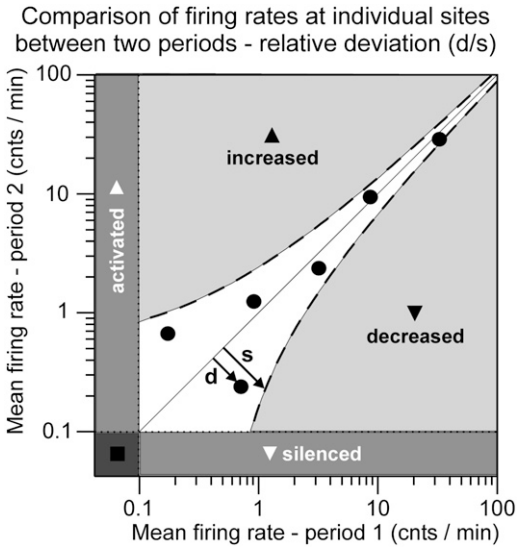

FIGURE 3 Comparison of mean firing rates (spikes per minute) at individual sites belonging to two measurement periods of spontaneous activity. Data points around the diagonal indicate sites with similar firing rates for both periods. The diagonal is complemented with a confidence region bounded by three SD in the firing rate, calculated for a Poisson distributed spike train. The boundaries were obtained by calculating for each point on the diagonal with coordinate (x, y), i.e., firing rates $x = y$, the points $(x + \Delta x, y - \Delta y)$ and $(x - \Delta x, y + \Delta y)$ of the lower and upper boundary, respectively, with $\Delta x = \Delta y = 3\sqrt{xT}/T = 3\sqrt{x/T}$ with T the duration of recording period. Outside the confidence region the scatterplot is divided into regions where sites are activated, silenced, increased, or decreased in firing rate. Sites with firing rates below 0.1 counts/min were considered inactive. The relative deviation of a data point from the diagonal is calculated by dividing the orthogonal distance between the data point and the diagonal (d) by the distance between the confidence boundary and the diagonal (s).

To quantify the amount of scatter in the scatter plots, the following measures were calculated for each experiment: the number of points in the region of activation, in the region of silencing, in the region of increased activity, in the region of decreased activity, and within the confidence region (Fig. 3). In addition, for each point in the scatter plot, the relative deviation (rd) from the diagonal was calculated by dividing the orthogonal distance (d_i) to the diagonal by the orthogonal 3 σ Poisson spread (s_i). This measure indicates how much the mean firing rate at that site has changed between the two periods compared. An rd value of 1 represents a point exactly on the 3 σ curve; values smaller than 1 are points within the 3 σ confidence region, and may indicate that the firing rate has not significantly changed. The more the rd value deviates from 1, the further away the point is from the 3 σ curve, and the bigger the difference in firing rate between the two periods compared. The mean rd (mrd) of each comparison was calculated by averaging over all data points in the scatter plot ($mrd = (1/N)\sum_i^N d_i/s_i$). The expected value of the relative deviation, $E(rd)$, for a normally distributed quantity is equal to $E(|x - \bar{x}|/3\sigma) = (1/3\sigma)\int_{-\infty}^{\infty} |x - \bar{x}|.g(x - \bar{x}, \sigma).dx = 0.266$, where $g(x - \bar{x}, \sigma)$ is a Gaussian function $g(x - \bar{x}, \sigma) = (1/\sigma\sqrt{2\pi})e^{-((x-\bar{x})^2/2\sigma^2)}$ with mean $\bar{x}$ and SD σ.

Return plots of individual large network burst profiles

The temporal evolution of the firing rates in individual network bursts was calculated and visualized using the method of Wagenaar et al. (22). Return plot orbits were constructed for each network burst. First, a window of maximally 1000 ms around the maximum of the network burst was defined. Within this window, the total number of spikes across all channels was determined by a sliding window that was slid in 1 ms time steps (Fig. 4). The bin width of the sliding window itself was 15 ms, 20 ms, or 35 ms, depending on the number of spikes and the width of the network burst. Then, a Gaussian smoothing was carried out (with a σ of 15 ms or 20 ms depending on the total number of spikes in the sliding window bins). Next, pairs of bin values were plotted as follows: the value of bin_i on the x axis and the value of bin_{i-d} on the y axis, where d stands for a delay. For the value of the delay, we took approximately half the width of the profile of the mean network. This procedure resulted in a smooth orbit for each network burst (see Fig. 11). Constructing orbits worked well for network bursts with a high number of spikes (bursts of: ~1200 spikes/s across all channels; duration: ~80 ms). For network bursts with fewer spikes and shorter duration, the orbits collapsed onto the origin of the axes. Orbits of large network bursts were plotted for the periods of 1 h before and 1 h after the stimulation session (see Fig. 11). To separate large network bursts from small ones, we first identified the network burst with the largest number of spikes at its center time. All networks bursts with a center-time value of at least 25% of this maximum value were then considered large network bursts.

RESULTS

Using dissociated cortical cultures grown on multielectrode arrays, we studied whether low-frequency electrical stimulation (0.2 Hz) can modify the stereotypical patterns of spontaneous activity in cortical neuronal networks. To this end, we analyzed spontaneous activity before and after a period of stimulation. Spontaneous activity of dissociated cortical cultures typically consists of periods of synchronized activity of many neurons, so-called network bursts, with low tonic activity, involving only several neurons, in between network bursts (11,12,27,28). We characterized both overall network activity and activity at individual electrode sites and in individual network bursts.

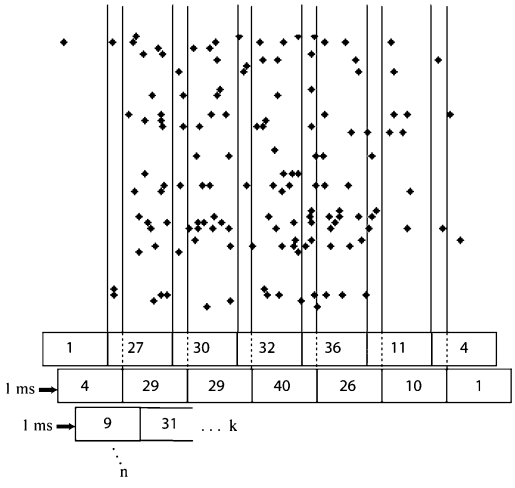

FIGURE 4 Illustration of return plot construction based on one network burst. Each dot represents a spike on a channel (*rows*). The duration of the network burst was divided into bins of a certain period and the total number of spikes across all channels was determined in every bin. After shifting all bins by 1 ms, the total number of spikes across all channels was determined again. This was continued until the end of the recording (containing any network bursts). The obtained array of spike amplitudes ($A(x)$) was then smoothed by convolving the array with a Gaussian. The smoothed array was then plotted in x, y coordinates (see Materials and Methods).

In Fig. 5 *A*, pieces of recordings are shown of spontaneous activity and 40 stimulus pulses (artifacts). The six traces correspond to the six stimulation sites. Pieces of spontaneous activity are shown before and after stimulation of each site. The figure shows that spontaneous networks bursts occur before, after, and during the stimulus train. Detailed inspection (Fig. 5 *B*) shows that the bursts during the stimulus train are not time locked to the individual stimulus pulses, but occur throughout the period between successive stimulus pulses.

We used four methods to quantify spontaneous activity before and after the stimulation session: 1), the mean firing rate in the whole culture; 2), the mean firing rate on individual electrode sites; 3), the shape of the profile of the mean network burst, and 4), the temporal structure of firing in large network bursts (see Materials and Methods for details).

Mean firing rate of the whole culture before and after stimulation

An example of the spontaneous firing activity in a culture 1 h before and 1 h after stimulation is shown in Fig. 6 *A*. In this example, the mean firing rate of the whole culture increased after stimulation due to an increase in the firing rates at several electrode sites (e.g., No. 7, No. 13, No. 40, No. 60). In other cultures, however, the total mean firing rate was found to decrease after stimulation. Considering all experiments, we did not find a systematic increase or decrease in mean firing rate or in the frequency of network bursts as a result of stimulation (Fig. 6 *B*).

Mean firing per electrode site before and after stimulation

To compare the spontaneous mean firing rates per electrode site before and after stimulation, we constructed scatter plots (Fig. 3; see Materials and Methods for details). Each point in the scatter plot represents the mean firing rate (spikes/min) at an individual electrode site. Three periods of spontaneous activity are compared in this way: the first versus the second half of the prestimulation period (Pre1–Pre2), the second half of the prestimulation period versus the first half of the poststimulation period (Pre2–Post1), and the first versus the second half of the poststimulation period (Post1–Post2). Fig. 7 shows examples of such plots for four cultures (rows).

The four examples in Fig. 7 illustrate that the scatter of data points in both the prestimulus and the poststimulus comparison is well within the fluctuations expected on the basis of a Poisson process. This observation underscores the stability of the firing rates in the prestimulus and the poststimulus period. The comparison between the pre- and poststimulus period, however, shows a markedly increased scatter, with many data points outside the Poisson region of confidence (see Materials and Methods), indicating changes in the firing rates at these recording sites after the period of stimulation. The increased scatter is also visualized by means of pie plots illustrating the fractions of sites (over all experiments) with decreased activity, increased activity, or no changes in activity (i.e., within the region of confidence; Fig. 8 *A*, see also Fig. 3). The plots illustrate that in the prestimulus–poststimulus comparison more data points fall above or below the region of confidence than in the prestimulus or in the poststimulus comparison.

The increased scatter is also reflected in the mean rd (*mrd*) values averaged over all experiments (i.e., the population *mrd*, or *pmrd*) (Fig. 8 *B*; see Materials and Methods for definition of *mrd*). The comparison of firing rates between successive 30-min periods both before and after the stimulus period resulted in a $pmrd = 0.56 \pm 0.07$ and $pmrd = 0.61 \pm 0.06$, respectively. The comparison between 30-min periods separated by an 80-min stimulus period resulted in $pmrd = 1.90 \pm 0.23$. We also carried out a number of control experiments ($n = 14$) with exactly the same durations of re-

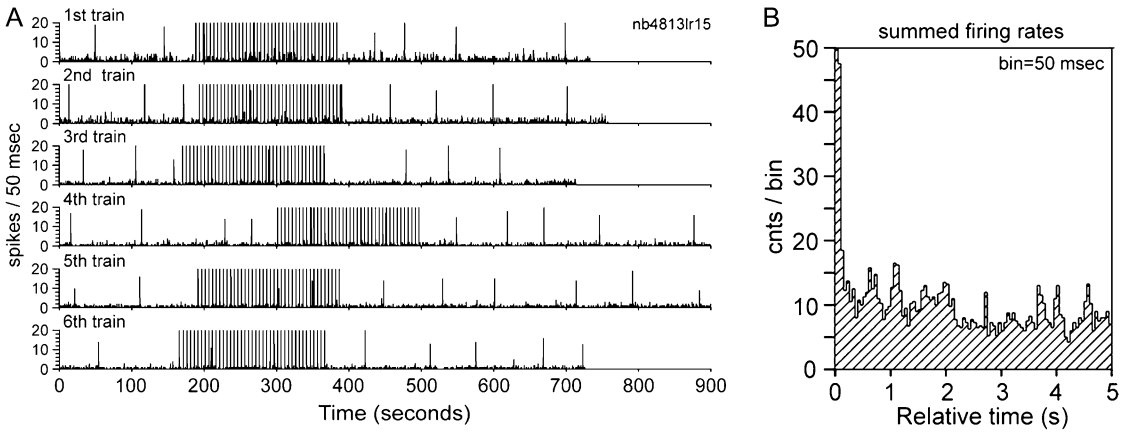

FIGURE 5 (*A*) Network-wide firing rates during a stimulation experiment. Each trace includes a period of spontaneous firing, a train of 40 0.2 Hz stimulus pulse artifacts (and evoked responses; not visible at the given time resolution) and again a period of spontaneous firing. The firing rate traces show the spontaneous network bursts and the low level firing in between. (*B*) Spike counts between two successive stimulus pulses, summed over 39 periods and six stimulus trains over all recording sites.

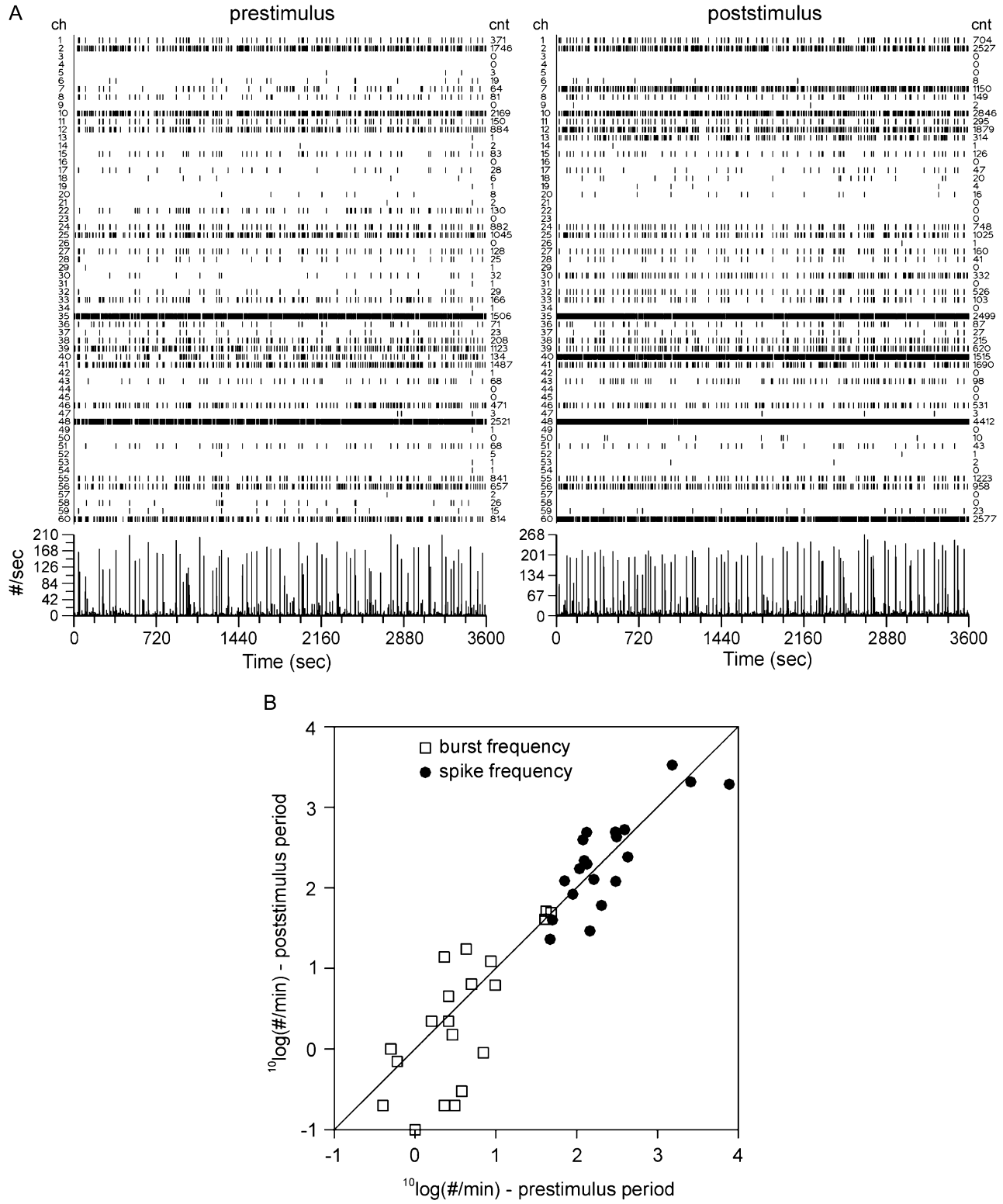

FIGURE 6 (*A*) Raster plots of spontaneous activity of 1 h before (*left*) and 1 h after (*right*) stimulation. Each trace corresponds to one recording electrode. The site index and the number of spikes measured are indicated at the left and right side of each trace, respectively. On the bottom *A*, histograms of the culture-wide firing rates are shown (time bin = 1 s). (*B*) Scatter plot of data points for all experiments, with each data point representing the mean total firing rate in spikes per minute (*solid circles*) or bursting frequency in bursts per minute (*squares*) in the period of 1 h before stimulation (*x* axis) and in the period of 1 h after stimulation (*y* axis).

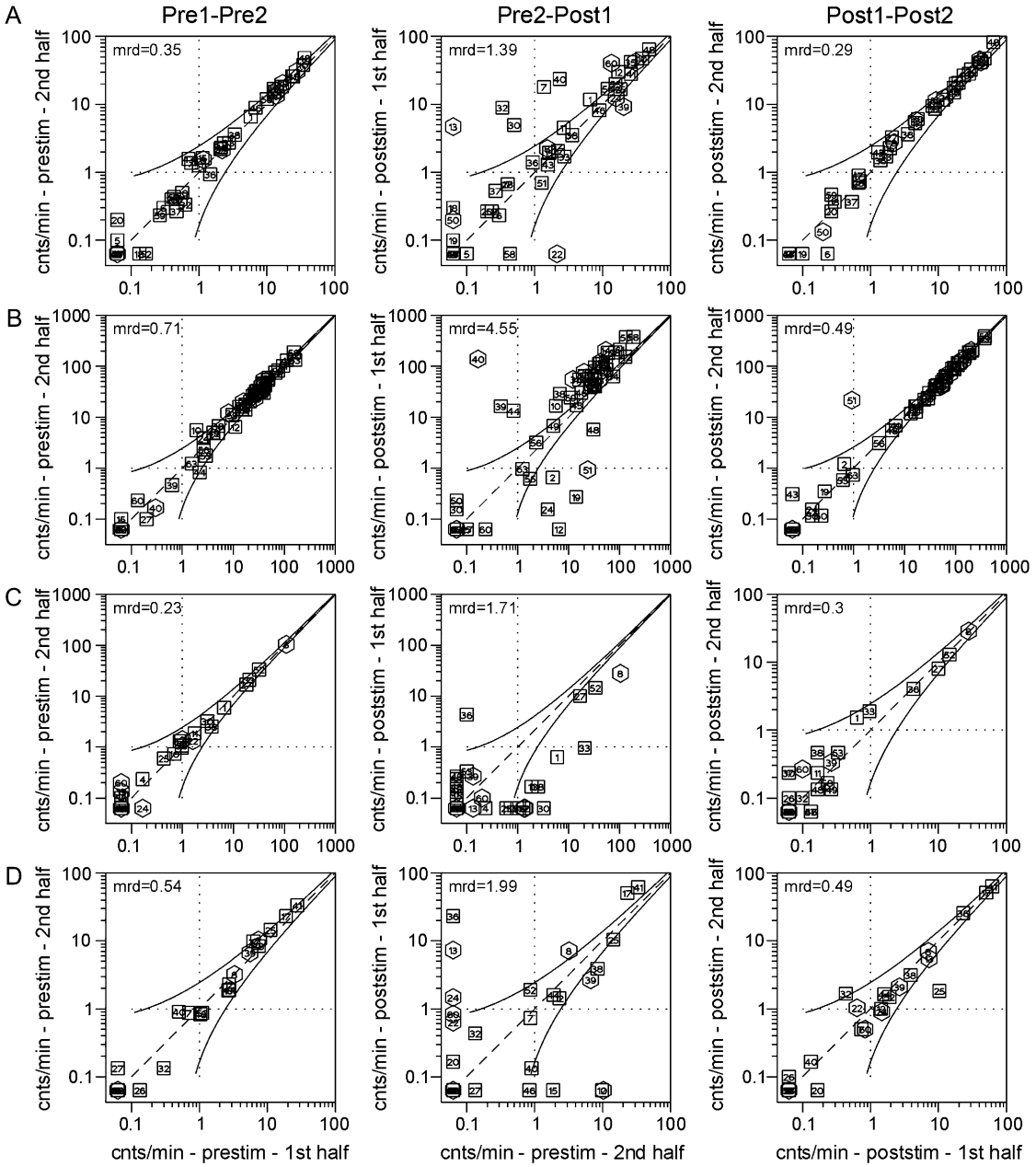

FIGURE 7 Spontaneous firing rates on individual sites of four cultures. Spontaneous activity was measured 1 h before and 1 h after the stimulation session. (*Left panels*) Comparisons between the first half and the second half of the 1 h spontaneous activity period before the stimulation session (Pre1–Pre2). (*Center panels*) Comparisons between the second half of the prestimulation period and the first half of the poststimulation period. (*Right panels*) Comparisons between the first and second halves of the 1 h spontaneous activity measurement after the stimulation session. Curved lines denote confidence intervals (for more explanation, see Materials and Methods and Fig. 3). *Mrd* values are indicated in the upper left corner of each panel.

cordings but without stimulating the culture. This means that the 80-min stimulation period was replaced by an 80-min control period in which we did not interfere with the culture. The comparison between successive 30-min periods before and after the 80-min control period resulted in an average scatter of $pmrd = 0.38 \pm 0.04$ and $pmrd = 0.30 \pm 0.02$, respectively. The comparison between 30-min periods separated by an 80-min control period resulted in $pmrd = 0.54 \pm 0.04$. Thus, all the comparisons between periods without stimulation in between (Fig. 8 *B*, bars a, c, a', b', and c') gave *pmrd* values well below one, indicating that the differences in firing rates are within the fluctuations expected on the basis of a Poisson process. In addition, these observed control values are quite close to the theoretically expected value of 0.27 for a Poisson process (see Materials and Methods). In contrast, the comparison with the stimulus period in between gave a *pmrd* value of 1.90, indicating that stimulation induced significant changes in the firing rates at individual electrodes (*t*-tests

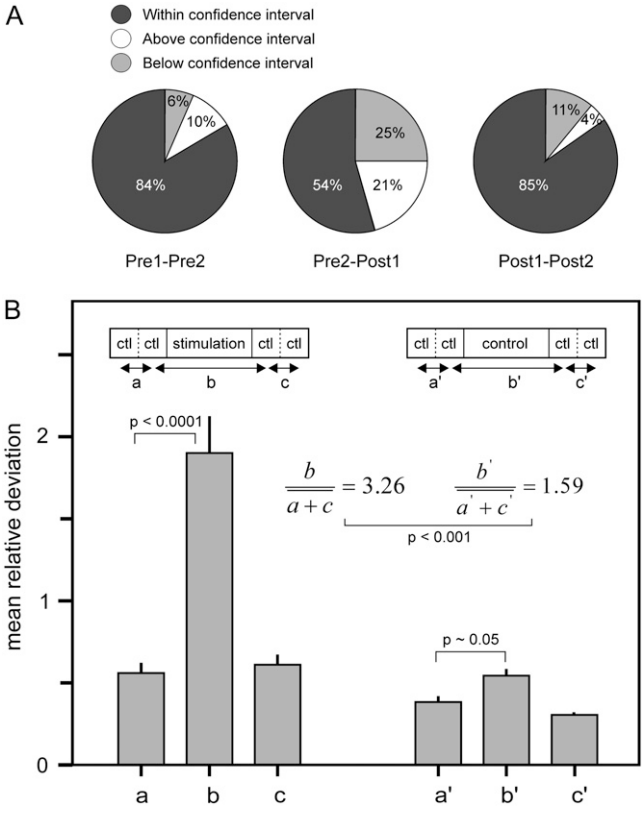

FIGURE 8 (*A*) Percentages of data points (sites) that fall within, below, and above the confidence interval in the firing rate scatter plots (Fig. 7). (*B*) Comparisons of firing rates between two periods of activity, expressed by the population average (*pmrd*) of the mean relative deviation (*mrd*) values over all experiments. The mean relative deviation quantifies the amount of scatter of data points in scatter plots comparing the firing rates in two periods. Comparisons were made between successive periods of 30 min before a period of stimulation (a, $pmrd = 0.56 \pm 0.07$, $n = 21$) or before a period of control recording (a', $pmrd = 0.38 \pm 0.04$, $n = 14$); between periods of 30 min separated by an 80 min period of stimulation (b, $pmrd = 1.90 \pm 0.23$, $n = 21$) or an 80 min period of control recording (b', $pmrd = 0.54 \pm 0.04$, $n = 14$); and between successive periods of 30 min after a period of stimulation (c, $pmrd = 0.61 \pm 0.06$, $n = 21$) or after a period of control recording (c', $pmrd = 0.30 \pm 0.02$, $n = 14$). The bars indicate mean values and SE. Bar b differs significantly from bars a and c (t-test, $p < 0.0001$). Bar b' differs slightly from bars a' and c' (t-test, $p \sim 0.05$). Bar b is 3.26 times the average of bars a and c. Bar b' is 1.59 times the average of bar a' and c'. These ratios differ significantly from each other ($p < 0.001$).

showed that bar a (Fig. 8 *B*) differs significantly from Fig. 8 *B*, bars b and c, with $p < 0.0001$).

In the control experiments, the comparisons between periods separated by an 80-min period without stimulation (Fig. 8 *B*, bar b') gave a somewhat larger scatter than the comparisons between successive periods (*bars* a' and c') with a t-test $p \sim 0.05$, also indicating that under control conditions firing rates at individual electrodes may slowly change. However, this change is much smaller than that induced by stimulation. Compared with the averages of the comparisons between successive periods, the scatter in the stimulation experiment is increased by a factor 3.26 ± 0.55 (in Fig. 8 *B*, bar b divided by the average of bars a and c), whereas in the control experiment it is only increased by a factor 1.59 ± 0.22 (bar b' divided by the average of a' and c'). t-Test statistics shows that these ratios differ significantly ($p < 0.001$). Thus, stimulation contributed significantly to the changes in the firing rates at the individual electrodes. The stability of the firing rates in the poststimulus period indicates that the new pattern of spontaneous activity is stable in the subsequent period of 1 h.

Mean network burst profile before and after stimulation

To identify a network burst, a bursting criterion was used (described in Materials and Methods). Individual network bursts were aligned to their center time, and spikes in a time window around the center time were summed and plotted in histograms with a bin width of 10 ms. A fitting procedure allowed us to define three characteristics of the mean network burst: the duration of its rising phase, the duration of its falling phase, and the duration of the whole network burst, defined as the sum of both (see Materials and Methods). In Fig. 9, four examples are given of mean network burst profiles during spontaneous activity measured before and after stimulation. In Fig. 9, both the profile of the mean network burst and the profile of the network burst per recording site are depicted. This latter visualizes the contribution of each electrode site to the mean network burst.

Fig. 9 shows that in some cultures, the rising phase and/or falling phase of the mean network burst has become shorter (Fig. 9, *A* and *D*) or longer (Fig. 9, *B* and *C*) as a result of stimulation. Activities at individual sites, which make up the network burst, also have changed after stimulation. Several changes can be observed: some active electrode sites become inactive (e.g., Fig. 9 *D*, *site 1*), some electrode sites that were inactive before stimulation become active (e.g., Fig. 9 *A*, *site 28*), some electrode sites increased their maximum firing level (Fig. 9, *B* and *C*), or have a more abrupt onset and offset of firing (Fig. 9 *D*).

In Fig. 10, the durations of the rising and falling phases of the mean network burst and their sum (i.e., the width of the network burst) are compared between prestimulus and poststimulus period (Fig. 10, *A–C*), and between two periods separated by a control period of 80 min (no stimulation) (Fig. 10, *D–F*). In each panel, the mean angle (*dashed line*) of the radius vectors of the data points (individual experiments) is plotted. We determined whether the angles of the radius vectors were significantly different from 45° (*solid line*). The means (SE) of these angles and the level of significance are 36.9 (2.6) ($p = 0.004$) for Fig. 10 *A*, 39.4 (2.6) ($p = 0.039$) for Fig. 10 *B*, 38.4 (2.5) ($p = 0.013$) for Fig. 10 *C*, 45.6 (1.4) ($p = 0.67$) for Fig. 10 *D*, 45.5 (1.6) ($p = 0.77$) for Fig. 10 *E*, and 45.3 (1.4) ($p = 0.84$) for Fig. 10 *F*. Thus, the angles of the mean radius vectors in Fig. 10, *A–C* are significantly smaller than 45°, indicating that mean network bursts after a period of stimulation have significant shorter rising phases, falling

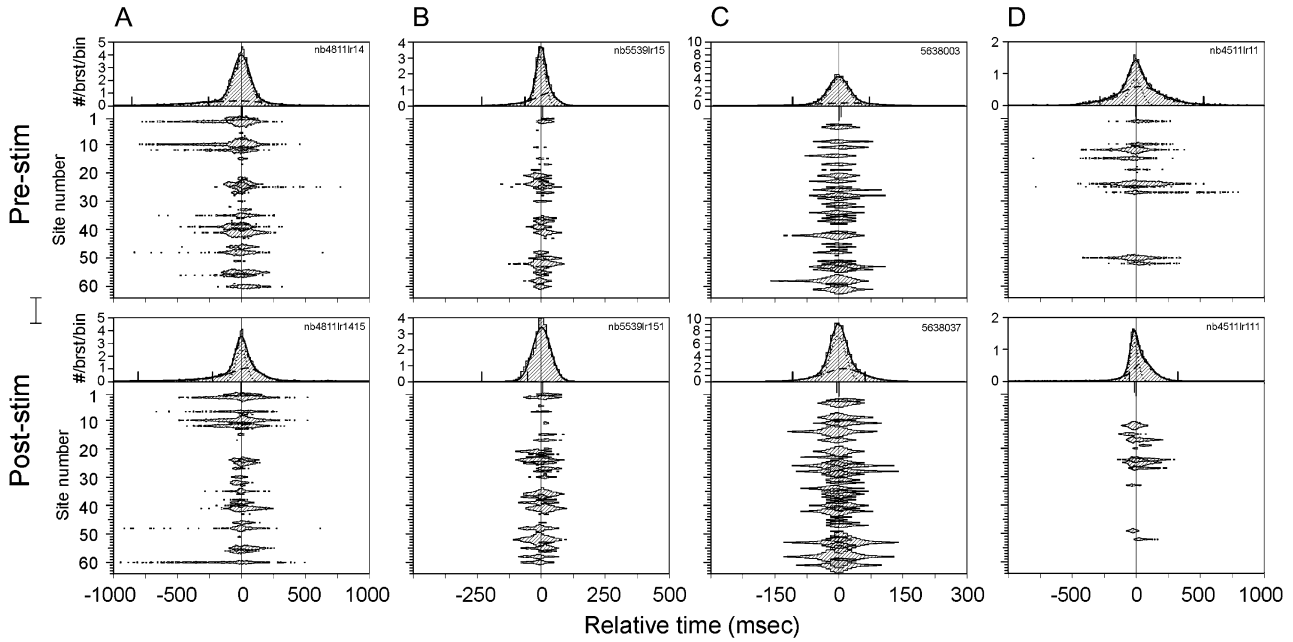

FIGURE 9 Network burst firing rate profiles obtained by averaging network bursts detected during a period of 1 h just before (*top row*) and just after (*bottom row*) stimulation in four experiments (*columns*). (*Upper panel part*) Mean firing rate during network bursts across all channels. (*Lower panel part*) Averaged firing rates per individual site, illustrating how each site differentially contribute to the total bursting activity. Left scale bar indicates a firing rate of one spike per site per network burst per time bin. The firing rates per individual sites are plotted symmetrically around their horizontal axes (note that frequencies smaller than 0.02 spikes per site per network burst per time bin have been omitted from the plot).

phases and total widths. No significant effects were found for the control data in Fig. 10, *D–F*, indicating that a control period of 80 min did not induce significant changes in these network burst parameters.

Temporal structure of firing in large network bursts before and after stimulation

To characterize the synchronous network firing in more detail, we have constructed return plots for individual network bursts. Return plots visualize the temporal evolution of the network-wide firing dynamics during individual network bursts (for a description of the construction of these plots see Materials and Methods and Fig. 4). Fig. 11 shows five examples of such return plots before and after stimulation.

The five cultures of Fig. 11 show that the size and shape of individual network burst orbits can change as a result of stimulation. Fig. 11, *A* and *C*, show cases in which both the size and the shape of the network bursts have changed. In other cases (Fig. 11 *B*, *D*, and *E*), only the size of the orbits is changed, whereas the overall shape of the orbits remains more or less the same. A smaller size of the orbits after stimulation indicates that there is less firing at the sites involved in the network bursts or that sites have been silenced altogether. A change in the shape of the orbits after stimulation points to an altered spatiotemporal structure of the network bursts. In summary, low-frequency stimulation changes the firing dynamics of individual network bursts, and this new pattern of stereotypic activity becomes stable in the period after stimulation.

DISCUSSION

Neuronal networks in the brain continually receive sensory input, while being intrinsically active themselves. Whether and how this intrinsic network activity is modified by the incoming inputs is largely unknown. We therefore examined how intrinsically active cortical neuronal networks in vitro would be affected by external stimulation. We stimulated dissociated cortical cultures grown on MEAs with low-frequency electrical stimuli and characterized the reverberating spontaneous network activity before and after stimulation. We quantified four major aspects of spontaneous network activity: the mean firing rate and the mean bursting rate in the whole culture, the mean firing rate on individual electrode sites, the shape of the mean network burst, and the temporal structure of firing in large network bursts.

Our main finding is that low-frequency stimulation changed the quantitative characteristics of spontaneous activity significantly and that this new activity pattern remained stable in the subsequent hour after stimulation. This is a novel and unexpected finding, because low-frequency stimuli have not yet been shown to cause lasting changes in the spatiotemporal pattern of spontaneous network activity. Low-frequency stimuli have been used mainly to probe cortical cultures, under the assumption that they do not themselves

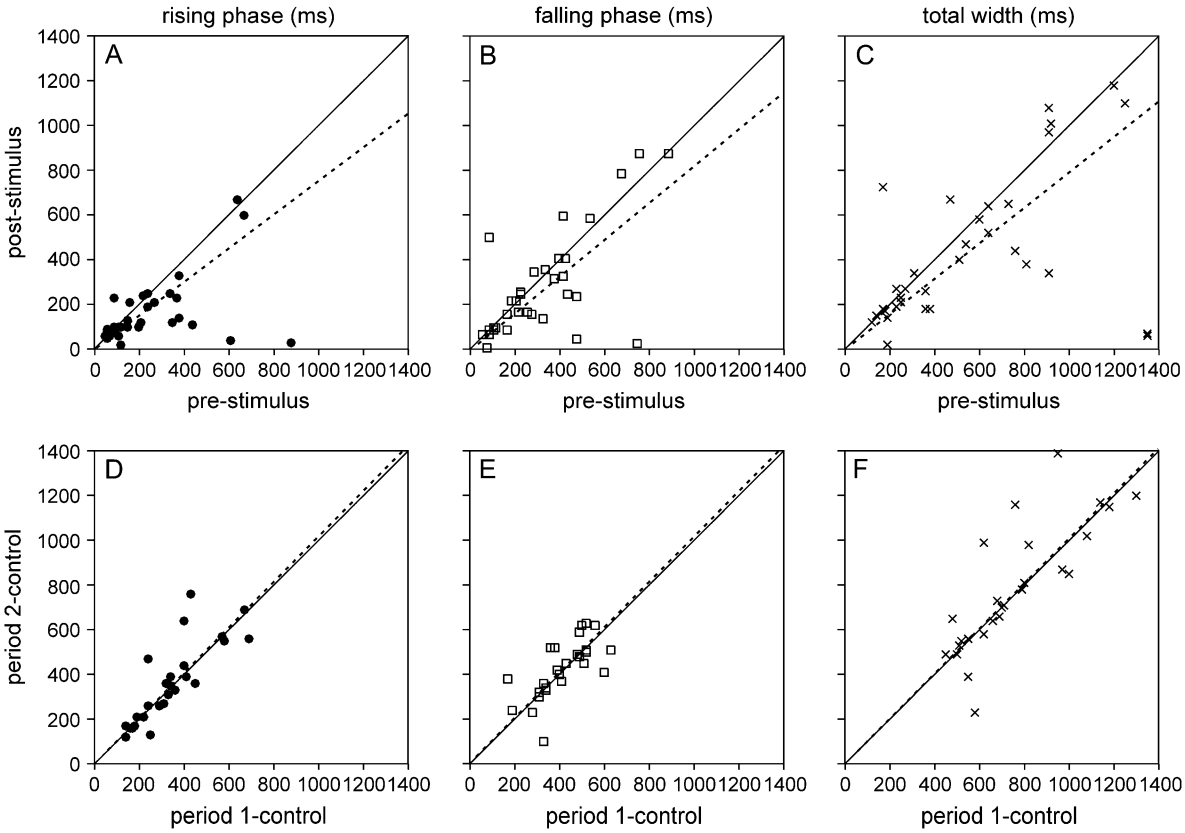

FIGURE 10 Comparison of network burst parameters between pre- and poststimulus period (*A–C*) and between two periods separated by a control period of 80 min (without stimulation) (*D–F*). (*A* and *D*) Rising phase. (*B* and *E*) Falling phase. (*C* and *F*) Total width. Each data point indicates one experiment. In each panel, the dashed line indicates the mean angle of the radius vectors of the data points, whereas the diagonal is drawn as a continuous line. The mean angles in *A*, *B*, and *C* are significantly smaller than 45°, indicating that network bursts after a period of stimulation have significantly shorter rise times, falling times, and total widths. The mean angles in *D*, *E*, and *F* do not differ significantly from 45°, indicating that a control period of 80 min did not induce systematic changes in these network burst parameters.

affect the spatiotemporal network activity (17,20,21). Clearly, this assumption does not hold, and changes in network activity induced by the probe stimuli themselves should be taken into account in future experiments.

All cultures showed significant and stable changes in activity pattern as a result of low-frequency stimulation, but the cultures differed with respect to how their activity was modified. After stimulation, culture-wide mean firing rate was either increased or decreased (Fig. 6). Frequency of network bursts showed a similar behavior: in some cultures the frequency of network bursts increased, whereas in others it decreased (Fig. 6). Likewise, mean firing frequencies on single electrode sites either increased or decreased (Fig. 7). Only the shape of the mean network burst after stimulation tended to change in a similar way across most cultures, with, on average, a shortening of the rising and falling phases of the network burst. Importantly, in all cultures the altered patterns of network activity did not keep on changing but were stable over time in the hour after stimulation.

Dissociated cortical cultures are mostly used to investigate the mechanisms governing cortical network development (11–13,18,26–28) or learning and memory (21,22,32). Only a few studies have dealt with stimulus-evoked activity in cortical cultures. Wagenaar et al. (16) looked at the most effective stimulation for evoking spikes. Tal et al. (33) studied the input-output relation of single neurons to various stimulation frequencies. Maeda et al. (18) applied external stimuli to study the properties of network burst propagation. Eytan et al. (19) examined adaptation to external stimuli. However, all these studies were concerned with relatively short-term effects of stimulation, at most several minutes after stimulus delivery. In our study, we were instead interested in the response of the cultures on a longer timescale. We recorded spontaneous activity and examined how this activity changed as a result of stimulation in the hour after stimulation. For this, we first analyzed the stability of the stereotypical network activity before stimulation. We thereby reproduced the findings of Shahaf and Marom (32) and Van Pelt et al. (11,27) that on timescales of several hours, spontaneous activity in dissociated cortical cultures is remarkably stable. This stability made it feasible to detect possible changes in spontaneous activity induced by stimulation.

How did low-frequency stimulation alter the pattern of spontaneous network activity in our cortical cultures? First,

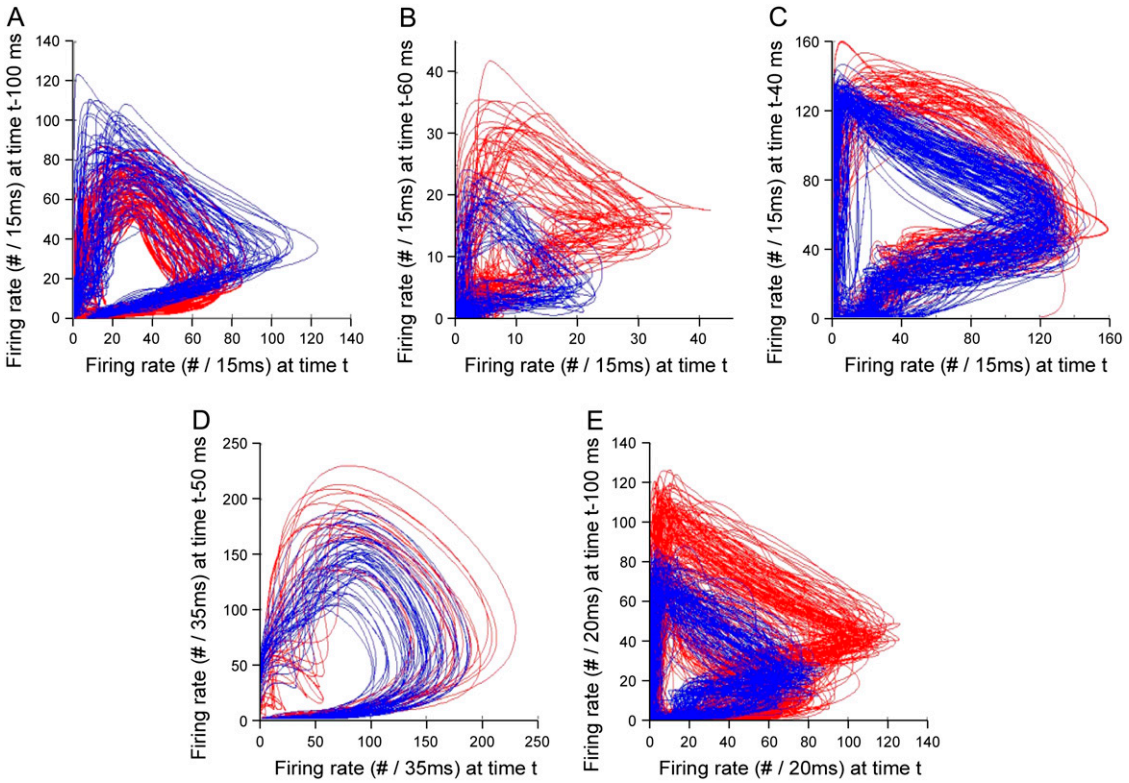

FIGURE 11 Return plots of the largest network bursts of five cultures before (*red*) and after (*blue*) the stimulation session. See Materials and Methods and Fig. 4 for explanation on the construction of the plots.

synaptic strengths may have been modified. The sharpening of the mean network burst profiles observed in almost all cultures may suggest that stimulation strengthened synaptic connections, leading to more strongly synchronized network activity. Enhanced network synchronization due to increased synaptic strength has been hypothesized to underlie the occurrence of high amplitude slow oscillations in the electroencephalogram of early sleep (34). Eytan et al. (19) suggest that the decrease in responsiveness they observed to 0.2 Hz stimulation is mostly a result of short-term synaptic depression. However, the same frequency (35) and even a higher frequency of 0.3 Hz (17,20,21) have been used as test stimuli before and after high-frequency tetanizing stimuli in learning studies in cortical networks, and thus were not assumed to change synaptic strengths, although this assumption was not directly examined. A second possibility is that low-frequency stimulation changed intrinsic neuronal properties, such as cellular-level excitability (36). Third, we may hypothesize that low-frequency stimulation did not modify synaptic strengths or intrinsic properties at all. As in neuronal network models with a fixed set of synaptic strengths and neuronal intrinsic properties (36) cultured cortical networks may have a number of different attractor states. A transition from one attractor to another can be accomplished by a temporary disturbance of activity, in our case provided by low-frequency stimulation on a number of electrode sites. Dissociated cortical cultures exhibit families of similar network bursts (10) and changes in network bursting have been interpreted as attractor state switches (22). Recently, hippocampal slice cultures (24) and in vivo hippocampal networks (22) have also been shown to exhibit attractor-like dynamics. Attractor state dynamics allows that stimulation can alter activity patterns without modification of synaptic strengths (37). Currently, we are testing this by repeating our experiments while synaptic plasticity is blocked.

We thank Elly van Galen and Ger Ramakers for making the cultures.

This work was supported by a European Union grant (NeuroBit project, IST-2001-33564) and by an Integrated Cognition Research Project grant from the Netherlands Organization for Scientific Research (NWO; grant NWOCOG/04-07).

REFERENCES

1. Buzsaki, G., and A. Draguhn. 2004. Neuronal oscillations in cortical networks. *Science*. 304:1926–1929.
2. Salenius, S., and R. Hari. 2003. Synchronous cortical oscillatory activity during motor action. *Curr. Opin. Neurobiol.* 13:678–684.
3. Varela, F., J. P. Lachaux, E. Rodriguez, and J. Martinerie. 2001. The brainweb: phase synchronization and large-scale integration. *Nat. Rev. Neurosci.* 2:229–239.
4. Kahana, M. J., D. Seelig, and J. R. Madsen. 2001. Theta returns. *Curr. Opin. Neurobiol.* 11:739–744.

5. Hoffman, K. L., and B. L. McNaughton. 2002. Coordinated reactivation of distributed memory traces in primate neocortex. *Science.* 297:2070–2073.

6. Hahn, T. T., B. Sakmann, and M. R. Mehta. 2006. Phase-locking of hippocampal interneurons' membrane potential to neocortical up-down states. *Nat. Neurosci.* 9:1359–1361.

7. Louie, K., and M. A. Wilson. 2001. Temporally structured replay of awake hippocampal ensemble activity during rapid eye movement sleep. *Neuron.* 29:145–156.

8. Harris, K. D. 2005. Neural signatures of cell assembly organization. *Nat. Rev. Neurosci.* 6:399–407.

9. Hebb, D. O. 1949. The Organization of Behavior. A Neuropsychological Theory. Wiley, New York.

10. Segev, R., I. Baruchi, E. Hulata, and E. Ben-Jacob. 2004. Hidden neuronal correlations in cultured networks. *Phys. Rev. Lett.* 92:118102.

11. Van Pelt, J., P. S. Wolters, M. A. Corner, W. L. Rutten, and G. J. Ramakers. 2004. Long-term characterization of firing dynamics of spontaneous bursts in cultured neural networks. *IEEE Trans. Biomed. Eng.* 51:2051–2062.

12. Wagenaar, D. A., J. Pine, and S. M. Potter. 2006. An extremely rich repertoire of bursting patterns during the development of cortical cultures. *BMC Neurosci.* 7:11.

13. Chiappalone, M., M. Bove, A. Vato, M. Tedesco, and S. Martinoia. 2006. Dissociated cortical networks show spontaneously correlated activity patterns during in vitro development. *Brain Res.* 1093:41–53.

14. Borg-Graham, L. J. 2001. Systems neuroscience: the slowly sleeping slab and slice. *Curr. Biol.* 11:R140–R143.

15. Corner, M. A., J. van Pelt, P. S. Wolters, R. E. Baker, and R. H. Nuytinck. 2002. Physiological effects of sustained blockade of excitatory synaptic transmission on spontaneously active developing neuronal networks–an inquiry into the reciprocal linkage between intrinsic biorhythms and neuroplasticity in early ontogeny. *Neurosci. Biobehav. Rev.* 26:127–185.

16. Wagenaar, D. A., J. Pine, and S. M. Potter. 2004. Effective parameters for stimulation of dissociated cultures using multi-electrode arrays. *J. Neurosci. Methods.* 138:27–37.

17. Wagenaar, D. A., J. Pine, and S. M. Potter. 2006. Searching for plasticity in dissociated cortical cultures on multi-electrode arrays. *J. Negat. Results Biomed.* 5:16.

18. Maeda, E., H. P. Robinson, and A. Kawana. 1995. The mechanisms of generation and propagation of synchronized bursting in developing networks of cortical neurons. *J. Neurosci.* 15:6834–6845.

19. Eytan, D., N. Brenner, and S. Marom. 2003. Selective adaptation in networks of cortical neurons. *J. Neurosci.* 23:9349–9356.

20. Tateno, T., and Y. Jimbo. 1999. Activity-dependent enhancement in the reliability of correlated spike timings in cultured cortical neurons. *Biol. Cybern.* 80:45–55.

21. Jimbo, Y., T. Tateno, and H. P. Robinson. 1999. Simultaneous induction of pathway-specific potentiation and depression in networks of cortical neurons. *Biophys. J.* 76:670–678.

22. Wagenaar, D. A., Z. Nadasdy, and S. M. Potter. 2006. Persistent dynamic attractors in activity patterns of cultured neuronal networks. *Phys. Rev. E.* 73:051907.

23. Wills, T. J., C. Lever, F. Cacucci, N. Burgess, and J. O'Keefe. 2005. Attractor dynamics in the hippocampal representation of the local environment. *Science.* 308:873–876.

24. Sasaki, T., N. Matsuki, and Y. Ikegaya. 2007. Metastability of active CA3 networks. *J. Neurosci.* 27:517–528.

25. Ramakers, G. J., J. Winter, T. M. Hoogland, M. B. Lequin, P. van Hulten, J. van Pelt, and C. W. Pool. 1998. Depolarization stimulates lamellipodia formation and axonal but not dendritic branching in cultured rat cerebral cortex neurons. *Brain Res. Dev. Brain Res.* 108:205–216.

26. Ramakers, G. J., F. C. Raadsheer, M. A. Corner, F. C. Ramaekers, and F. W. Van Leeuwen. 1991. Development of neurons and glial cells in cerebral cortex, cultured in the presence or absence of bioelectric activity: morphological observations. *Eur. J. Neurosci.* 3:140–153.

27. Van Pelt, J., M. A. Corner, P. S. Wolters, W. L. Rutten, and G. J. Ramakers. 2004. Longterm stability and developmental changes in spontaneous network burst firing patterns in dissociated rat cerebral cortex cell cultures on multielectrode arrays. *Neurosci. Lett.* 361:86–89.

28. Van Pelt, J., I. Vajda, P. S. Wolters, M. A. Corner, and G. J. Ramakers. 2005. Dynamics and plasticity in developing neuronal networks in vitro. *Prog. Brain Res.* 147:173–188.

29. Chiappalone, M., A. Novellino, I. Vajda, A. Vato, S. Martinoia, and J. van Pelt. 2005. Burst detection algorithms for the analysis of spatio-temporal patterns in cortical networks of neurons. *Neurocomputing.* 65–66:653–662.

30. Press, W. H., S. A. Teukolsky, W. T. Vetterling, and B. P. Flannery, editors. 1992 Numerical Recipes in FORTRAN, The Art of Scientific Computing, 2nd ed. University Press, Cambridge, UK.

31. Eytan, D., and S. Marom. 2006. Dynamics and effective topology underlying synchronization in networks of cortical neurons. *J. Neurosci.* 26:8465–8476.

32. Shahaf, G., and S. Marom. 2001. Learning in networks of cortical neurons. *J. Neurosci.* 21:8782–8788.

33. Tal, D., E. Jacobson, V. Lyakhov, and S. Marom. 2001. Frequency tuning of input-output relation in a rat cortical neuron in-vitro. *Neurosci. Lett.* 300:21–24.

34. Tononi, G., and C. Cirelli. 2006. Sleep function and synaptic homeostasis. *Sleep Med. Rev.* 10:49–62.

35. Van Staveren, G. W., J. R. Buitenweg, E. Marani, and W. L. C. Rutten. 2005. The effect of training of cultured neuronal networks, can they learn? *Intl. IEEE EMBS Conf. on Neural Engineering*. Arlington, VA.

36. Zhang, W., and D. J. Linden. 2003. The other side of the engram: experience-driven changes in neuronal intrinsic excitability. *Nat. Rev. Neurosci.* 4:885–900.

37. Hopfield, J. J. 1982. Neural networks and physical systems with emergent collective computational abilities. *Proc. Natl. Acad. Sci. USA.* 79:2554–2558.